Postharvest Biology and Technology 207 (2024) 112633

Contents lists available at ScienceDirect

Postharvest Biology and Technology

journal homepage: www.elsevier.com/locate/postharvbio

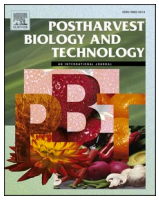

Citral enhances disease resistance in postharvest citrus fruit through inducing jasmonic acid pathway and accumulating phenylpropanoid compounds

Bin Duan [a,1], Okwong Oketch Reymick [a,b,1], Zhaoguo Liu [a], Yun Zhou [a], Xin Wang [a], Zhao Feng [a], Nengguo Tao [a,*]

[a] School of Chemical Engineering, Xiangtan University, Xiangtan, Hunan 411105, PR China
[b] Department of Science, Technical and Vocational Education, Makerere University, P.O BOX 7062, Kampala, Uganda

ARTICLE INFO

Keywords:
Citral
Jasmonic acid pathway
Induced resistance
Citrus fruit
Transcriptomics
Metabolomics

ABSTRACT

Citral, a monoterpene naturally present in volatile oils of *Litsea cubeba, Cymbopogon flexuosus* and citrus peel, can enhance disease resistance in postharvest citrus fruit and reduce fruit decay due to *Penicillium digitatum*. To clarify the defense mechanism involved in the enhancement of disease resistance, RNA-seq, metabolomics and biochemical analyses were integrated to global change in citral-treated fruit. Results showed that citral fumigation was effective at controlling citrus green mold. Citral increased the activities of phenylalanine ammonia-lyase, peroxidase, and polyphenol oxidase, followed by elevated contents of total phenolics, flavonoids, and lignin. Metabolomics revealed that citral treatment triggered accumulation of the plant hormones methyl jasmonate, abscisic acid, and indoleacetic acid, and many phenylpropanoid metabolites including curcumin, cinnamyl alcohol, hesperidin, syringin, 7-methoxyflavonol, vitexin-2-O-rhamnoside, coniferin, naringin, kaempferol-7-neohesperidoside, and *trans*-cinnamaldehyde. RNA-seq results revealed that the expression levels of multiple genes involved in jasmonic acid (JA) profiles and phenylpropanoid biosynthesis were markedly upregulated by citral. These findings suggest that the JA pathway is positively involved in the induced disease resistance of citrus fruit by citral, and provide a novel theoretical support by which citral fumigation manages postharvest citrus green mold.

1. Introduction

Citrus is a sort of bulk fruit owing to its excellent taste, refreshing flavor, and its high content of ascorbic acid, phenolic compounds and flavonoids (Singh et al., 2020). *Penicillium digitatum* is a necrotrophic phytopathogen that infect citrus fruit through the wounds on surface of the fruit and leads to establishment of green mold, which causes significant economic losses worldwide (Bhatta, 2022). Currently, green mold is mainly controlled by commercial chemical fungicides (Chen et al., 2019). With increased consumer awareness and concerns about food safety and environmental pollution due to chemical fungicides, essential oils (EOs) gained extensive interest as a means to extend fruit shelf life. This is attributed to their superior antimicrobial characteristic and ability to trigger fruit resistance against pathogenic fungi (El Khetabi et al., 2022; He et al., 2016). Thus, environment-friendly EOs have gradually come into researchers' perspective for postharvest diseases control in fruit and vegetables.

Citral, normally present in *Litsea cubeba, Cymbopogon flexuosus,* and citrus EOs, is a natural monoterpene (Luciano et al., 2023; Tamer et al., 2019). It has been gradually used to control deterioration of fruit and vegetables for its characteristic lemon-like flavor, antioxidant, and antimicrobial properties (Tamer et al., 2019). It was previously reported to exhibit strong antifungal activity against some fungi in postharvest citrus like *P. italicum*, *P. digitatum*, and *Geotrichum citri-aurantii* (Wuryatmo et al., 2014). Citral also induced host resistance against some plant fungi like *Erysiphe cucurbitacearum*, *Botrytis cinerea*, and *Sclerotinia sclerotiorum* (Jiang et al., 2022). We previously reported that wax+citral was effective at reducing green mold incidence by triggering disease resistance in Ponkan fruit, as evidenced by increase in the activities of the antioxidant enzyme catalase (CAT), superoxidase dismutase (SOD),

* Corresponding author.
E-mail address: nengguotao@126.com (N. Tao).
[1] These two authors contributed equally to this work.

https://doi.org/10.1016/j.postharvbio.2023.112633
Received 26 June 2023; Received in revised form 12 October 2023; Accepted 21 October 2023

and peroxidase (POD) (Fan et al., 2014). However, the underlying molecular mechanism that mediates resistance response is not clearly understood and needs further investigations.

Induced resistance is an effective strategy to control diseases by eliciting and regulating biochemical processes in fruit and vegetables (Prusky and Romanazzi, 2023). The capacity of EOs to trigger fruit defense responses and reduce their physiological deterioration has broadly been investigated (El Khetabi et al., 2022). Generally, the activation of fruit defense response by EOs mainly concentrates on maintenance of redox balance, accumulation of antifungal substances, improvement of antioxidant capacity and enhancement of defense-related enzymes, etc. (Yousuf et al., 2021). For example, Li et al. (2020) reported that tea tree oil enhances the resistance of strawberry fruit against *Botrytis cinerea* by enhancing phenylalanine ammonia-lyase (PAL), cinnamate-4-hydroxy lase (C4H), 4-coumarate-CoA ligase (4CL), POD, and polyphenol oxidase (PPO) activities, as well as accumulating flavonoids, coumarin and phenolic compounds. (E)- 2-hexenal fumigation reduced disease severity of kiwifruit gray mold by upregulating expression level of mitogen-activated protein kinase and genes encoding pattern recognition receptors, and promoting the biosynthesis of jasmonic acid (JA) and flavonoids in the kiwifruit (Hyun et al., 2022). In citrus fruit, clove EOs effectively controlled blue mold by improving the production of H_2O_2 and increasing the activities of PAL, POD, PPO, β-1,3-glucanase (β-Glu), chitinase (CHI), and lipoxygenase (LOX) in Xinyu tangerine (Chen et al., 2019). EOs blend composed of cinnamaldehyde, carvacrol and eugenol also reduced spoilage of orange by inhibiting growth of *P. digitatum*, reducing hydrogen peroxide accumulation and stimulating phenylpropanoid metabolism in navel orange (Yang et al., 2022).

Jasmonates, composed of free acid JA and methyl jasmonate (MeJA), are a prerequisite for inducing fruit resistance against pathogens. Studies in strawberries, sweet cherries and tomatoes demonstrated that their defense response against pathogens were all through activation of JA biosynthesis and signaling (Li et al., 2021; Li et al., 2022; Min et al., 2022). Exogenous addition of MeJA can also activate resistance of apple and sweet cherry by enhancing the activities of defense-related enzymes and promoting accumulation of antifungal compounds (Pan et al., 2022; Zhao, et al., 2022). Additionally, treatment with compounds like chitosan can also stimulate increased expression of genes associated with JA biosynthesis to enhance grape resistance to *B. cinerea* attack (Zhang et al., 2021). However, it is unclear if citral induces the disease resistance of citrus fruit by triggering the JA pathway.

This study therefore, aimed at investigating the mechanism by which citral enhanced citrus fruit resistance to *P. digitatum* to control the establishment of green mold decay. The potential regulatory pathways and key metabolites were investigated by RNA-Seq and metabolomic. Further, the roles of the JA pathway and the phenylpropanoid biosynthesis in citral-induced citrus resistance were also explored by genetic and biochemical levels.

2. Materials and methods

2.1. Fruit, chemical and pathogen

Mature citrus fruit (*Citrus unshiu* Marc. cv. Miyagawa Wase) were harvested from an orchard in Xiangtan city, Hunan Province, China, on November 5th, 2021. The initial color index, total solids content (TSS) and titratable acid (TA) of selected citrus fruit were 2.24, 11.92% and 10.89%, respectively. All fruit were rapidly delivered to the laboratory and spread on a clean surface for 24 h to release the field heat. Fruit consistent in size, color and with no injury or infection were selected for the subsequent experiments.

Citral (97%) was purchased from Macklin (Shanghai, China). *P. digitatum* was provided the laboratory and prepared as described by Duan et al. (2021).

2.2. Evaluation of the effects of citral on the artificially inoculated infection in citrus fruit

Fruit were rinsed thrice in distilled water after being sterilized with 2% sodium hypochlorite for 2 min and then air-dried. Two symmetrical wounds were (3 mm × 3 mm) made on opposite sides of the fruit equator using a sterilized stainless blade, and inoculated with 10 μL of *P. digitatum* spore suspension (1×10^6 conidia mL^{-1}). The inoculated fruit were randomly placed in four cartons (26 cm × 14.5 cm×18.5 cm) fumigated with citral of concentration 0, 50, 100, or 200 μL L^{-1}. Two holes were punched on opposite sides of each carton to allow for free air circulation. Materials that carried citral were fixed to the inner top surface of the carton while avoiding direct contact with the fruit. All inoculated citrus fruit were kept at 25 °C and 85–90% relative humidity (RH) for 6 d. Disease incidence and lesion diameter were assessed on days 3, 4 and 5 (Duan et al., 2021). Fruit whose decay diameter exceeded 3 mm were classified as infected as described by Duan et al. (2018).

2.3. Evaluation of ability of citral to induce disease resistance in citrus fruit

The sterilized citrus fruit were subjected to vapor treatment with 100 μL L^{-1} citral before inoculation. On 3 d and 4 d after fumigation, fruit were left at 25 °C for 1 h to allow the evaporated citral to adsorb to their surface. The pretreated fruit were inoculated with 10 μL of the *P. digitatum* conidial suspension. Fumigation, storage of the fruit and data statistics were performed as detailed in Section 2.2 above. Fig. 1 is an operation diagram to illustrate the stages involved in fruit treatment with citral.

2.4. Sample collection

Citrus fruit were fumigated with 100 μL L^{-1} citral and stored at 25 ± 2 °C with 85–90% RH. Peel samples were collected from the tissue at

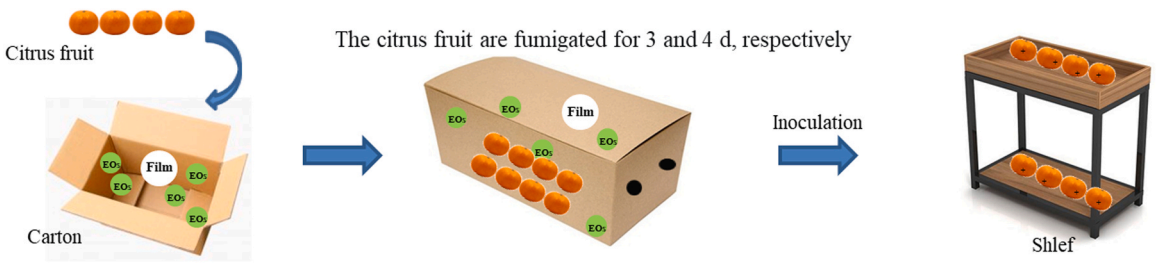

Fig. 1. Diagramatic illustration of the stages in EOs (citral) treatment.

equatorial region of the healthy fruit at 0, 12 h, 1, 2, 3, 4, 5, and 6 d. The samples were immediately frozen in liquid nitrogen and kept at − 80 °C ready for the subsequent transcriptomic, metabolomic, and biochemical analyses. Each treatment was replicated thrice, each replicate consisting of 10 fruit at each time point.

2.5. Measurement of enzyme activities and secondary metabolites

PAL, POD, PPO, total phenolics, flavonoids and lignin were determined according to Duan et al. (2021). The PAL, POD, and PPO activities were expressed as U kg^{-1} based on fresh weight (FW), where U= 0.01 OD_{290} h^{-1}, U = 0.01, OD_{470} min^{-1}, and U = 0.01 OD_{420} min^{-1}, respectively. Total phenolics and lignin were expressed as ΔOD_{280} kg^{-1} based on FW. Flavonoids was expressed as ΔOD_{325} kg^{-1} based on FW. Each treatment consisted of three parallel experiments.

2.6. Metabolomic analysis

On the basis of the maximum induction of the total phenolics and flavonoids, 100 mg of peels (control and citral treatment) sampled on 3 d were selected for metabolomic analysis (Leng et al., 2022; Wang et al., 2020). Each treatment included six replicates. Data preprocessing, filtering and statistical analysis were conducted by Bioprofile Biotechnology Co., Ltd, Shanghai, China. The procedures were the same as described previously (Wang et al., 2017). To match the altered metabolic pathways, the differential metabolite data was analyzed using Kyoto Encyclopedia of Genes and Genomes (KEGG) (http://www.kegg.jp) and Human Metabolome database (HMDB) (https://hmdb.ca/metabolites). KEGG analyses were conducted using Fisher's exact test, and False Discovery Rate (FDR) correction for multiple testing.

2.7. Transcriptomic analysis

Basing on the results of the activities of PAL, POD and PPO, we found that resistance at transcriptional level had begun at 12 h. So, one gram of citral-treated and control peel samples from the 12 h treatment were used for transcriptome sequencing. Each treatment included three replicates. RNA extraction, library construction, sequencing, and data processing were conducted by Personalbio Technology Co., Ltd, Shanghai, China. The procedures were the same as described previously (Gong et al., 2022). The sequencing library was then sequenced on NovaSeq 6000 platform (Illumina). Differential gene, gene ontology (GO) and KEGG enrichment were conducted according to Wang et al. (2023) and Zhang et al. (2019). The differentially expressed genes (DEGs) were annotated using the GO database (http://www.geneontology.org) and KEGG to analyze the differentially expressed genes (DEGs) with DESeq (1.30.0), Blast2GO suite and ClusterProfiler (3.4.4) software.

2.8. Determination of gene expression encoding JA biosynthesis and signaling pathway

Total RNA was extracted from the control and citral-treated peels by Plant Total RNA Kit (Zoman, Beijing, China). RNA quality and integrity were assayed using a spectrophotometry (TGem Pro, Tiangen, Beijing, China) and agarose gel electrophoresis, respectively. The total RNA (1 μg) was used for cDNA synthesis using Hifair® III 1st Strand cDNA Synthesis SuperMix for qPCR (gDNA digester plus) (Yeasen, Shanghai, China). Then, diluted cDNAs were used for real-time qPCR (RT-qPCR) by a LightCycler96 system (Roche, Basel, Switzerland), following the instructions of the Hieff UNICON® Universal Blue qPCR SYBR Master Mix (Yeasen, Shanghai, China). The suitable primers (Table S1) of the target genes were designed by Primer Premier 6.0 software. The relative expression of the genes was normalized to the *Actin*, and calculated using the $2^{-\Delta\Delta Ct}$ method (Livak and Schmittgen, 2001). Three biological replicates were performed for each sample.

2.9. Determination of JA and MeJA contents

JA and MeJA were extracted and measured according to the previous method (Zhi and Zhang, 2013) by using an enzyme-linked immunosorbent assay Kit (Enzyme-linked, Shanghai, China) with a Sunrise™ enzyme-labeled instrument (Tecan, Grodig, Austria). The contents of JA and MeJA were performed by the Kit instructions, and expressed as μg kg^{-1} based on FW.

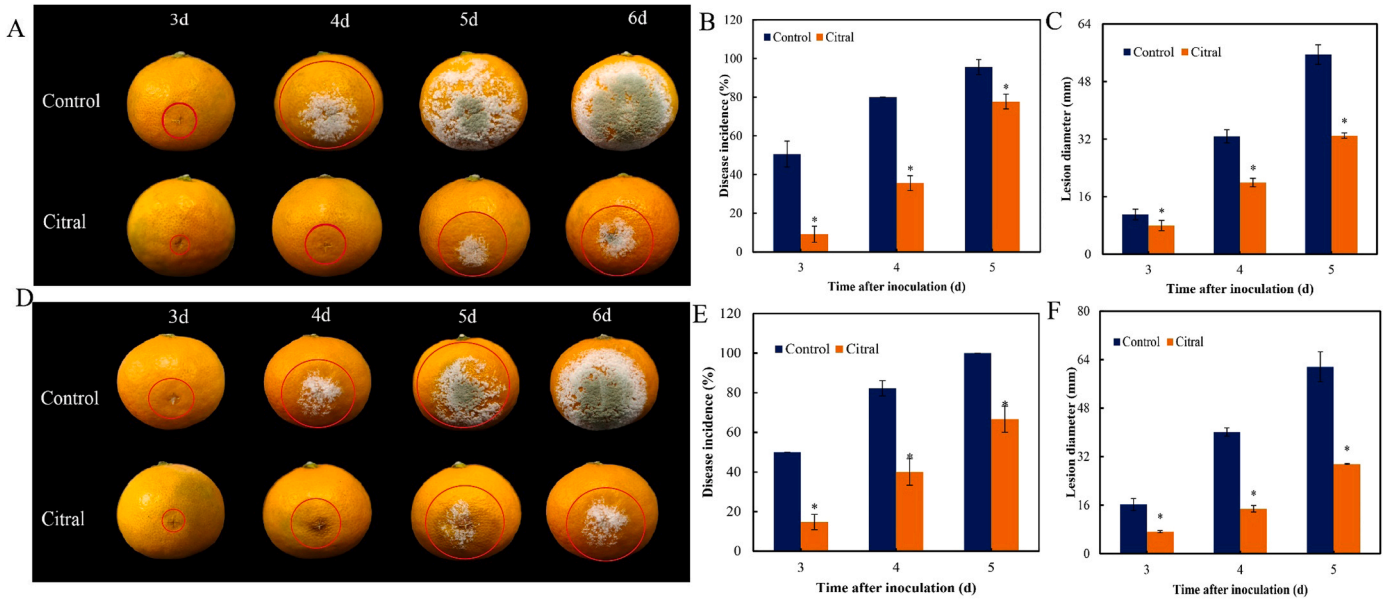

Fig. 2. Effect of citral at 100 μL L^{-1} treatment on induced resistance of citrus fruit inoculated with *P. digitatum*. Visual appearance of green mold disease on fruit treated with citral after 3 d (A) or 4 d (D) of pre-exposure. Each wound was inoculated with 10 μL of a 1 × 10^6 spores mL^{-1} spore suspension. Disease incidence (B, E) and lesion diameter (C, F) of citrus fruit pre-exposed to citral for 3 d and 4 d, respectively. Values are presented as means ± SD (n ≥ 3). Asterisks indicate significant differences ($p < 0.05$) between control and citral-treated citrus fruit within the same storage time.

2.10. Statistical analysis

Results were presented as average ± standard deviation and analyzed using SPSS 19.0 (SPSS, Inc., Chicago, USA) software. A one-way analysis of variance (ANOVA) and independent two-sample t-test were used to count significant differences between citral-treated and control samples at $p < 0.05$. The relationship visualization was constructed using STRING (https://string-db.org/) database and R package.

3. Results

3.1. Citral exposure inhibited the green mold development in citrus fruit

Citral fumigation at three concentrations (50, 100, and 200 μL L^{-1}) effectively reduced green mold decay during fruit storage (Fig. S1). Particularly, fruit exposure to 100 μL L^{-1} citral led to the least disease incidence and lesion diameter as compared the other treatments. By 5 d of incubation, all fruit in the control group were completely rotten yet only 52.8% of the 100 μL L^{-1} citral treated fruit were colonized. Similarly, the lesion diameter in the citral-treated fruit was only 33.5 mm, which was lower than that in the control fruit (58.3 mm). These results indicate that citral at an optimum concentration of 100 μL L^{-1} effectively controlled establishment of green mold disease in citrus fruit, and excessive concentration of citral might lead to fruit toxicity, thus reducing the effectiveness of disease control.

3.2. Citral fumigation induced disease resistance of postharvest citrus fruit

Pretreatment of citrus fruit with citral markedly limited disease development in infected fruit (Fig. 2). For the fruit pre-exposed with citral for three days, all control fruit were fully colonized by 5 d, while only 66.67% of the 100 μL L^{-1} citral treated fruit were colonized. The

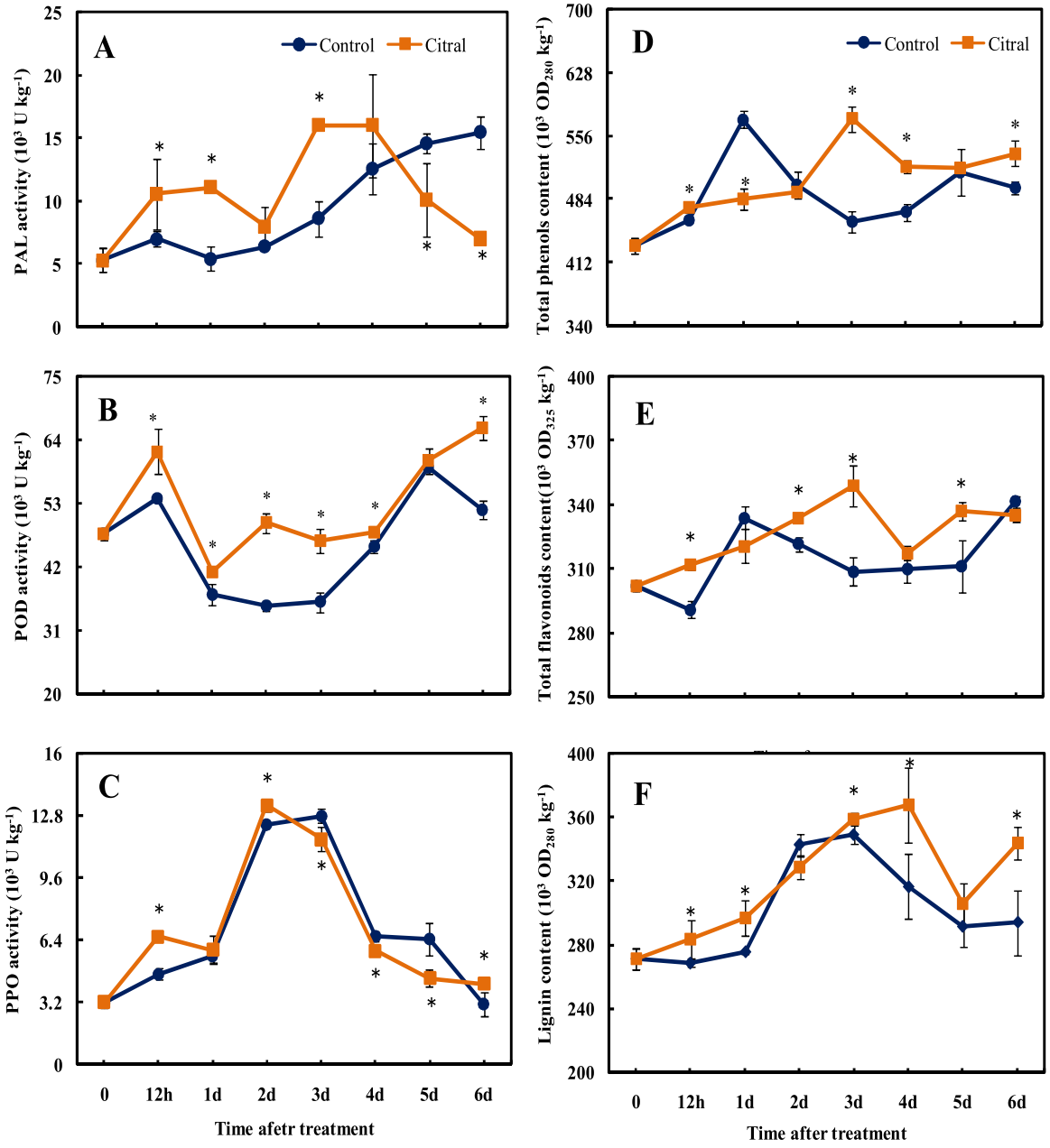

Fig. 3. Changes in enzyme activities and content of secondary metabolites in citrus fruit fumigated with 100 μL L^{-1} citral. A: PAL activity; B: POD activity; C: PPO activity; D: total phenolic; E: total flavonoids; F: lignin contents. Values are presented as means ± SD (n ≥ 3). Asterisks indicate significant differences ($p < 0.05$) between control and citral-treated citrus fruit within the same storage time.

corresponding lesion diameter of the citral-treated fruit were lower than those of the control fruit (Fig. 2C and D). Semblable phenomenon was observed in fruit pre-treated with citral for four days. However, green mold disease ensured on 3 d in the citral-treated fruit with a disease incidence of only 9.07%, which was markedly lower than the 55.7% in the control fruit. Correspondingly, fruit that received citral pretreatment had much lower lesion diameters (Fig. 2E and F). On 5 d after inoculation, the lesion diameter of fruit in the citral group was 29.6 mm, which was approximately half of the 61.6 mm in the untreated group.

3.3. Citral increased enzyme activities and secondary metabolites in the phenylpropanoid pathway

We also examined the activities of the enzymes PAL, POD and PPO (Fig. 3). PAL activity was higher in citral-treated samples than in the control samples before 4 d. The activity increased with increase in time, reaching a peak value 85.2% higher than in control samples on 3 d. POD activity showed double peaks in the citral-treated fruit peels, one at 12 h and the other on 6 d. The values were always higher in the test fruit relative to the untreated samples, except on 5 d. PPO activity showed a similar pattern in both treated samples. The activity gradually increased

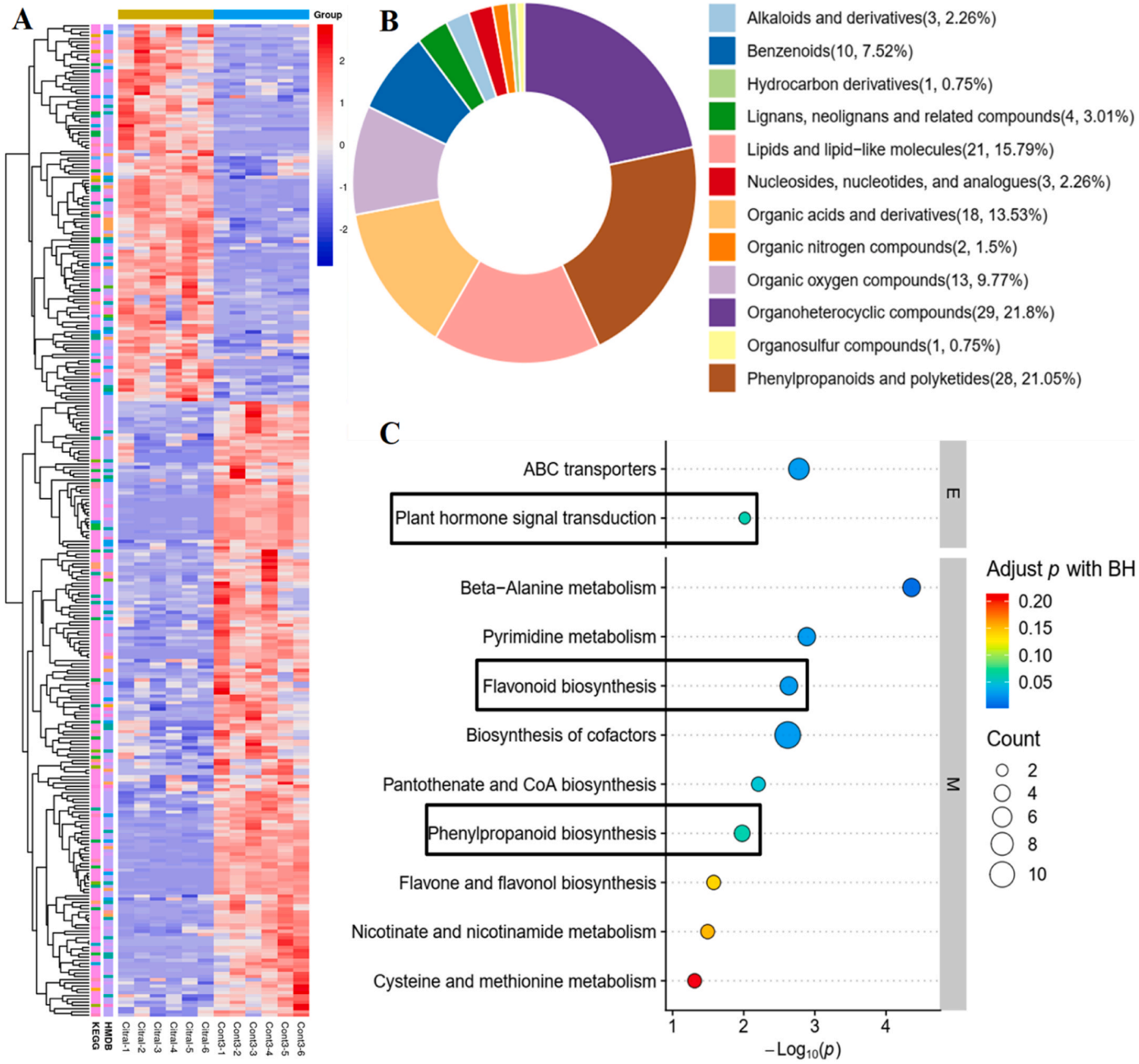

Fig. 4. Widely targeted metabolomics analysis in citrus fruit treated with citral. (A) Cluster analysis of metabolites from samples. Each row in the color heat map represents a single metabolite. The levels of metabolites were plotted in a heat map on the $\log_{10}$ scale. (B) Pie chart depicting the biochemical classification of the different expressed metabolites DEMs identified between the control and citral-treated groups. (C) Bubble diagram of the metabolic pathway enrichment analysis. The X-axis enrichment factor is the number of DAMs annotated to this pathway divided by all identified metabolites annotated to this pathway. The higher the value, the higher the ratio of DAMs annotated to this pathway. Dot size represents the number of DAMs annotated to this pathway. Cont3 represents control samples at 3 d.

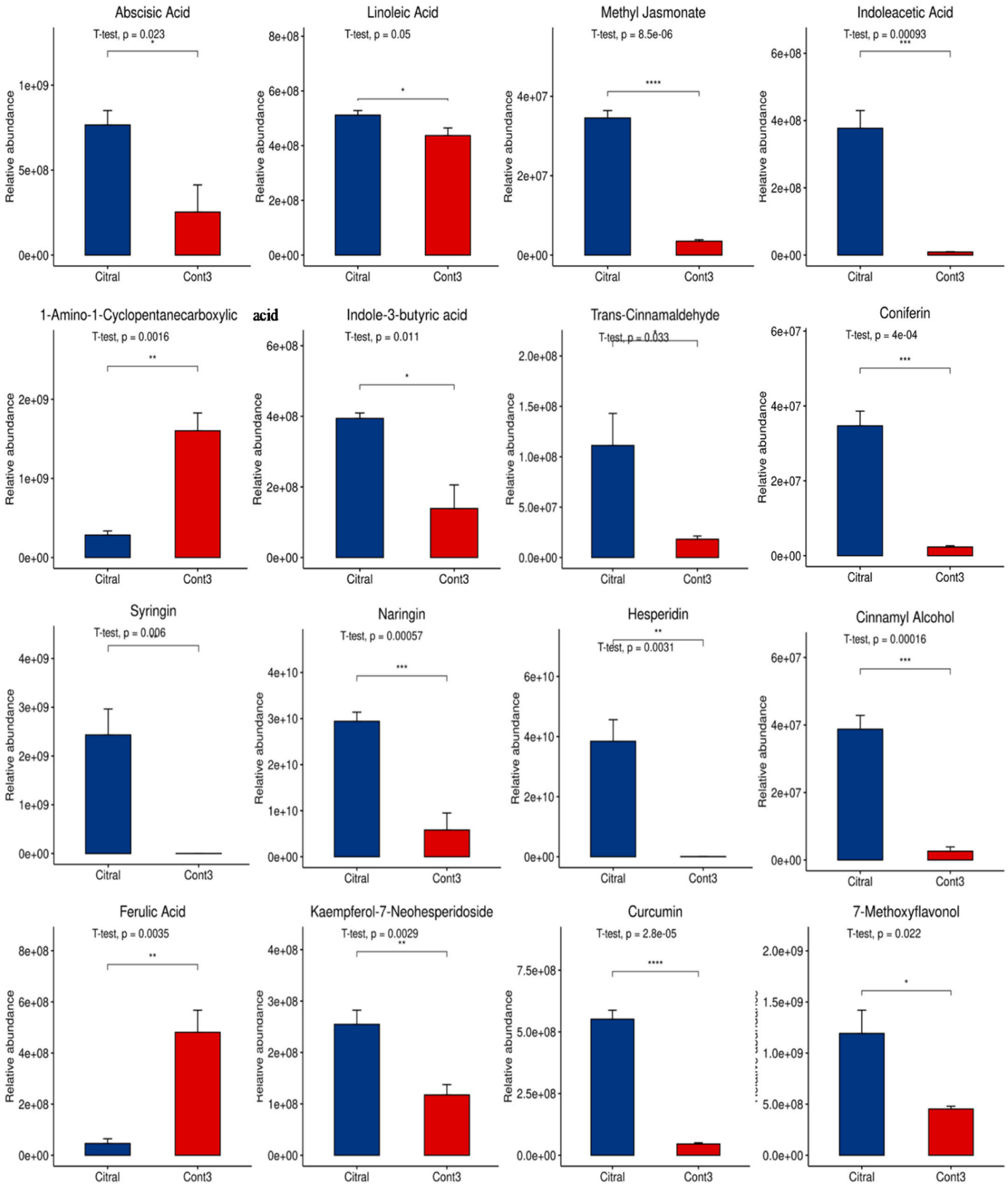

Fig. 5. Key differentially accumulated plant hormones and secondary metabolites in citrus peels treated with citral of concentration 100 μL L^{-1}. Values shown here are from the average of three biological replicates. Asterisks above the bar indicate significant differences among the different treatments at $p < 0.05$. Cont3 represents control samples at 3 d.

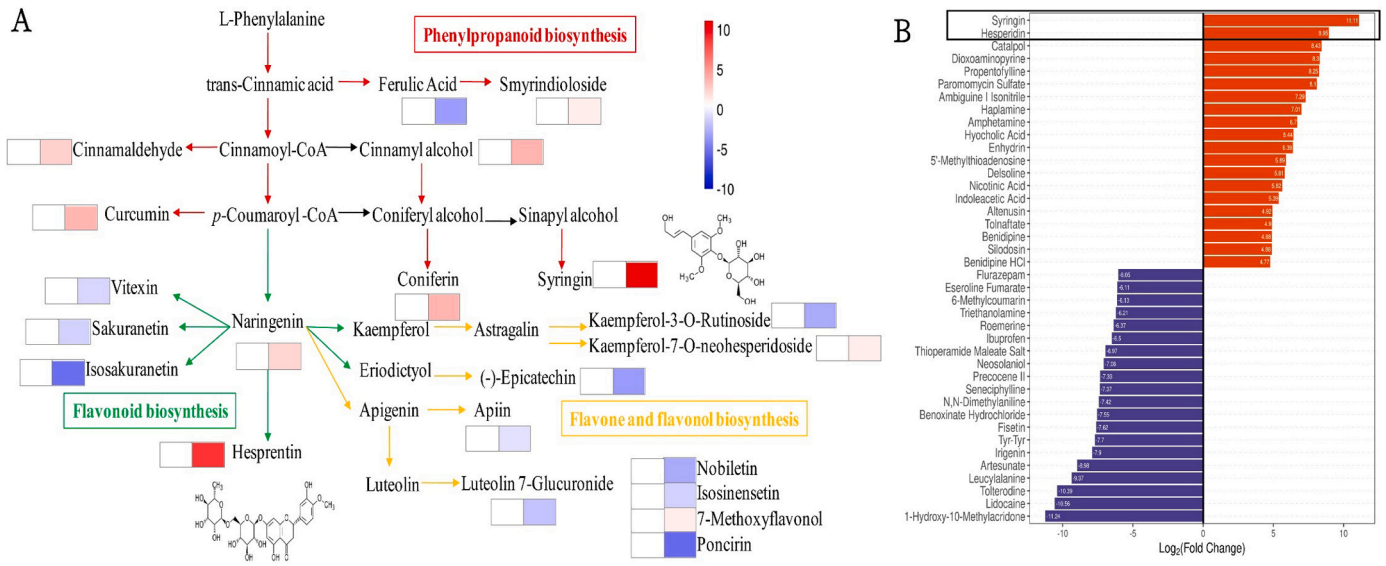

Fig. 6. (A) Metabolic pathway analysis of differentially accumulated metabolites involved in phenylpropanoid metabolism in citral-treated citrus fruit. (B) Fold change bar diagrams of the top ranked differential metabolites. Data are presented as a $\log_2$ value compared to control group. The red color indicates an increase, while blue indicates a decrease.

in both citral-treated and control samples to maximum values on 2 d and 3 d, respectively, before declining to minimum values. Compared to the control samples, high PPO activity was recorded in citral-treated peels at 12 h, and on 2 d and 6 d. Beyond that, the value was lower than in the control samples.

The changes in total phenols, flavonoids and lignin were evaluated in the citral-treated and control samples (Fig. 3D-F). Total phenols and flavonoids increased in the citral-treated fruit to reach peaks on 3 d then declined. The values at the peaks were respectively 25.5% and 44.9% higher than those in the control groups. In contrast, contents of total phenols and flavonoids in control samples peaked on 1 d and then decreased to values lower than in the citral-treated samples. Except for 2 d, the lignin content in citral-treated peels were markedly higher than that in the control samples throughout the storage period. On 4 d, the value reached a peak, which was 16.1% higher than that in the control samples. Overall, citral fumigation induced disease resistance of the postharvest citrus fruit against *P. digitatum*.

3.4. Metabolic profile of citrus fruit treated with citral

To comprehensively understand the metabolite changes in citral treated citrus peels, an untargeted metabolome profiling of peels from fruit within the test- and control samples was performed. The metabolomic data of citral-treated and control samples were evaluated by partial least squares discriminant analysis (PLS-DA), R2Y and Q2Y values, and the results showed that a good reproducibility of the metabolite model (Fig. S2). In total, 308 differentially accumulated metabolites (DAMs) were identified and listed in Supplementary data 1. Hierarchical cluster heatmap showed distinct metabolic patterns between citral-treated and untreated groups (Fig. 4A). These DAMs could be categorized into 12 classes, the main ones being organ heterocyclic compounds, phenylpropanoids and lipids (Fig. 4B), which accounted for 21.80%, 21.05% and 15.79% of total DAMs, respectively. These DAMs showed that they were mainly categorized into beta-alanine metabolism, pyrimidine metabolism, ABC transporters, flavonoid biosynthesis, pantothenate and CoA biosynthesis, plant hormone signal transduction, phenylpropanoid biosynthesis, flavone and flavonol biosynthesis (Fig. 4C). Notably, phenylpropanoid, flavonoid, plant hormone, flavone and flavonol were closely associated with enhancement of fruit resistance.

Within the DAMs involved in plant hormones signal transduction, the contents of linolenic acid, abscisic acid, indole-3-butyric acid, indoleacetic acid, MeJA rapidly increased after citral treatment (Fig. 5). In particularly, the relative amount of MeJA in citral-treated peels was 9.86-fold higher than that in the control group. When we analyzed the contents of MeJA and JA in the citral-treated samples using a microplate reader, the content of MeJA showed double peaks throughout the storage period (Fig. S3). The peak value in citral treated samples was elevated on 1 d and 3 d, being 14.0% and 15.3% higher than the values in the respective control samples. The result on 3 d was particularly consistent with our metabolomics, reaffirming the reliability of our metabolomic data. Additionally, compared to the control samples, exposure of fruit to citral increased accumulation of endogenous JA (Fig. S3B).

The content of secondary metabolites also increased within citral-treated peels. Majority of these were phenolics and flavonoids produced by the phenylpropanoid pathway. We further analyzed the key metabolites that are potential contributors to disease resistance in citral treated samples (Fig. 6). A total of 31 phenylpropanoid-related metabolites were identified in citral-treated citrus peels. Eleven of these metabolites namely coniferin, hesperidin, naringin, syringin, 7-methoxy flavonol, kaempferol-7-neohesperidoside, curcumin, *trans*-cinnamaldehyde, cinnamyl alcohol, camellianin, and vitexin-2-O-rhamnoside were upregulated. Notably, citral fumigation considerably induced accumulation of syringin and hesperidin, whose $\log_2$FC values reached 11.11 and 8.95, respectively (Fig. 6B). This signified that they were potential contributors to the enhancement of disease resistance. These results also implied that JA biosynthesis and phenylpropanoid pathway might participated in citral-induced resistance enhancement in citrus fruit.

3.5. RNA-seq analysis revealed key pathways mediating citral-conferred citrus fruit resistance

To understand the underlying regulatory mechanisms in the citral-treated citrus fruit, samples at 12 h of exposure were used for the high-throughput transcriptome sequencing by Illumina sequencing. Raw reads ranging from 36472934 to 45933318 were obtained in six samples, and approximately 92% of clean data were mapped to the citrus *unshiu* genome (Table S2). Q20 values were all greater than 96% in the citral-treated and control samples. Pearson's correlation

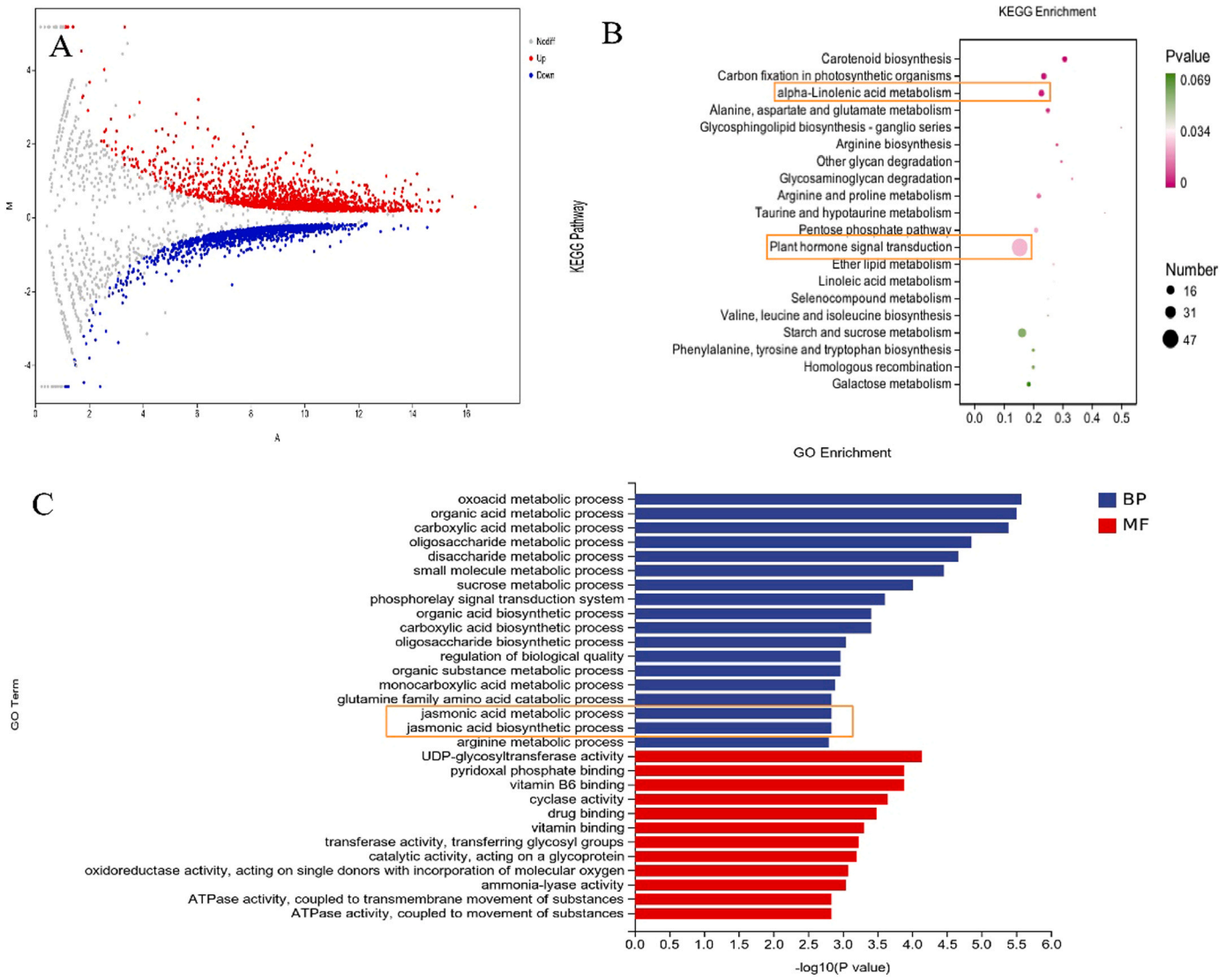

Fig. 7. Transcriptional analysis of citrus fruit treated with citral. (A) Number of DEGs that were up-regulated (red) and down-regulated (blue) in citral-treated citrus fruit. (B) Results from GO term. The number of significantly enriched DEGs within most GO divisions is shown. The color gradient, ranging from pink, through white, to green represents low, middle and high *p*-values over the course of the storage period. (C) Results from KEGG enrichment analysis for DEGs. The color gradient indicates different *p*-value.

coefficient (r) analysis confirmed that the transcriptome data were high quality and reliability (Fig. S4).

In total, 1668 and 1266 DEGs were up-regulated and down-regulated in citral-treated peels, respectively (Fig. 7A). Cluster analysis of the six samples was used to compare the expression patterns between samples as evidenced by the color distribution (Fig. S5). In total, 259 GO terms were enriched and the top 30 terms are shown in Fig. 7C. They were mainly enriched in molecular function and biological process, such as: metabolic process related to oxoacid, organic acid, carboxylic acid, oligosaccharide, disaccharide, UDP-glycosyltransferase activity, pyridoxal phosphate binding and vitamin B6 binding. Notably, jasmonic acid metabolic and biosynthetic processes were significantly enriched in GO terms. Meanwhile, KEGG enrichment database showed that 1034 DEGs were categorized into 122 pathways (Fig. 7B). Among them, 15 pathways were significantly enriched in citral-treated citrus fruit. These included carotenoid biosynthesis, alpha-linolenic acid metabolism, alanine, plant hormone signal transduction, glycosphingolipid biosynthesis and arginine biosynthesis (Fig. 7B). Strikingly, numerous DEGs involved in alpha-linolenic acid metabolism and plant hormone signal transduction were greatly enriched in citral-treated samples, which highly correlated to JA biosynthesis and signaling.

3.6. *Citral exposure promoted JA biosynthesis and signaling*

Multiple genes involved in JA biosynthesis were markedly upregulated in the citral treated fruit (Fig. 8). These included *OPC-8:0 CoA ligase 1* (*OPCL1*), *hydroperoxide lyase* (*HPL*), *acyl-CoA oxidase* (*ACOX*), *acetyl-CoA acyltransferase 1* (*ACAA1*), four *LOX*, *allene oxide synthase 1* (*AOS1*), three *allene oxide cyclase* (*AOC*), three *12-oxophytodienoate reductase* (*OPR*) and *jasmonic acid carboxyl methyl transferase* (*JMT*). In addition, *coronatine-insensitive protein 1* (*COI1*), four *jasmonate-ZIM domain* (*JAZ*) and three *transcription factors MYC2* involved in JA signaling were also upregulated (Fig. 8A). To verify the actual role of the JA pathways in citral treatment, eight genes (*LOX2–1*, *AOS1*, *AOC*, *OPR11*, *JMT*, *COI1*, *JAZ1*, and *MYC2*) were selected for qRT-PCR (Fig. 8B-I).

Fig. 8 disclosed that the expression levels of above-mentioned genes were influenced by citral treatment. The expression levels of *LOX2–1*

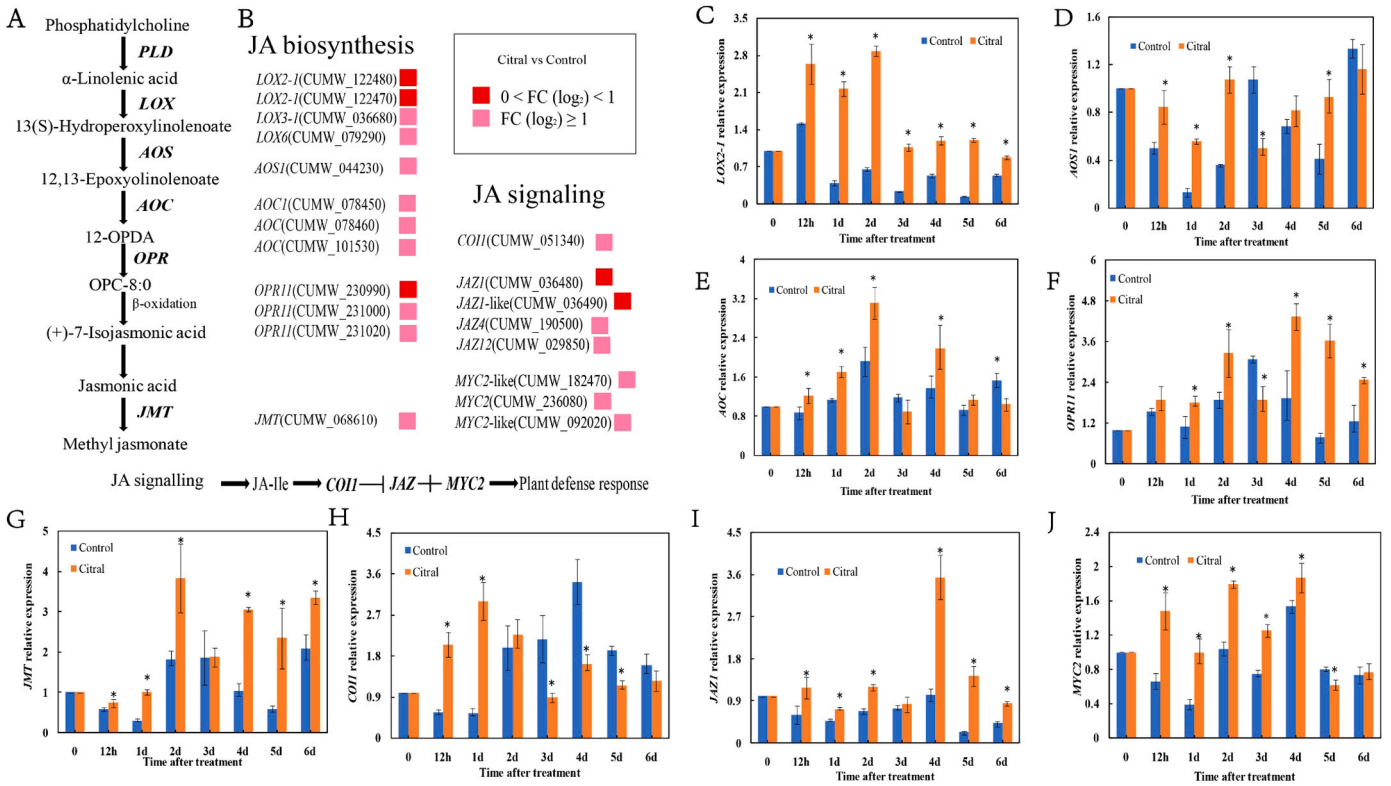

Fig. 8. Variations of citral treatment on expression patterns of DEGs involved in JA pathway. Expression patterns of JA biosynthesis and responsive genes (A, B) after citral treatment. In the heatmap, different colors indicate changes in expression levels between citral-treated and control samples. The color gradient, ranging from brown, through white, to green represents low, middle and high expression levels after citral treatment. qRT-PCR (C-J) verified the expression profiles of selected JA pathway related DEGs after citral treatment. The values were presented as means ± SD. Asterisks indicate significance of differences ($p < 0.05$) between citral-treated and control groups.

increased in the citral-treated samples, exhibiting a dramatic rise on 2 d, to a level 4.41-fold higher than in the control samples (Fig. 8B). The expression level of *AOS1* in the citral-treated samples increased at 12 h, on 1 d, 2 d and 5 d, relative to the control group. Citral treatment enhanced the peak of *AOS1* on 2 d to levels 3.01- fold higher than in the control group (Fig. 8C). Similarly, citral exposure also enhanced the expression of *AOC* to a peak 1.62-fold higher than in control fruit on 2 d (Fig. 8D). Other than day 3 of treatment, the expression levels of *OPR11* were always higher in citral-treated samples than in the corresponding control samples. A maximum expression, 2.24-times higher than that in the control samples was recorded on 4 d (Fig. 8E). Expression of *JMT* in citral-treated peels followed a similar pattern as that of *AOS1*. A value twice higher than that in the control samples was recorded on 2 d (Fig. 8F). Compared to the control samples, expression of *COI1* in the citral treatment group was greatly enhanced before 2 d, and subsequently inhibited after 3 d (Fig. 8G). *JAZ1* was highly expressed in the citral-treated peels all through the treatment period. A spike in expression level, 3.45 times higher than in control samples was recorded on 4 d (Fig. 8H). Similarly, *MYC2* was highly expressed in citral-treated peels than in control group before 4 d. Beyond 4 d, its expression level was approximately the same as in control group (Fig. 8I). The qRT-PCR results at 12 h were consistent with the RNA-seq data, confirming the reliability of transcriptome sequencing, and indicating that JA pathway in the citrus peel were activated by citral treatment.

3.7. Modulation of citral fumigation on phenylpropanoid pathway

We also screened out multiple genes involved in phenylpropanoid biosynthesis (Fig. 9). A total of 33 phenylpropanoid biosynthesis-related genes were found including *PAL*, *4CL*, *cinnamoyl-CoA reductase* (*CCR*), *shikimate O-hydroxycinnamoyl transferase* (*HCT*), *acetylserotonin O-methyltransferase* (*COMT*), *POD*, *cinnamyl-alcohol dehydrogenase* (*CAD*), *coniferyl-alcohol glucosyltransferase* (*UGT72E*), *chalcone synthase* (*CHS*), *flavanone 3-hydroxylase* (*F3′H*), *flavonol synthase* (*FLS*) and *flavonol 7-O-beta-glucosyltransferase* (*UGT71C4*). Compared with control group, the expression levels of these genes were all induced by citral. Furthermore, three genes that function as phenol oxidases were also identified including *laccase 17(LAC17), LAC7* and *LAC13,* which are all implicated in the oxidation of phenolic compounds.

3.8. Interaction network analysis of genes after citral fumigation

To reveal the potential interrelationships between the various genes previously mentioned, interaction network analysis of JA biosynthesis, signaling, and phenylpropanoid biosynthesis genes were performed (Fig. 10). The genes involved in JA biosynthesis or signaling showed highly positive relations with phenylpropanoid biosynthesis-related genes. We found that three genes including *MYC2*, *COI1*, *AOS1* were the center of the co-expression network and possessed 26, 25, 29 regulatory relations, respectively, indicating that they might be crucial in the citral treated JA pathway. Moreover, they positively correlated with the phenylpropanoid biosynthesis genes, including *PAL*, *PAL2*, *PAL-like*, and *4CL5*. Overall, JA biosynthesis and signaling, and phenylpropanoid biosynthesis genes might interact to improve disease resistance of postharvest citral-treated citrus fruit.

4. Discussions

Essential oils (EOs) have become vital alternatives to synthetic fungicides, and gained widespread attention due to their ability to reduce decay and maintain fruit quality after harvesting (Yousuf et al., 2021).

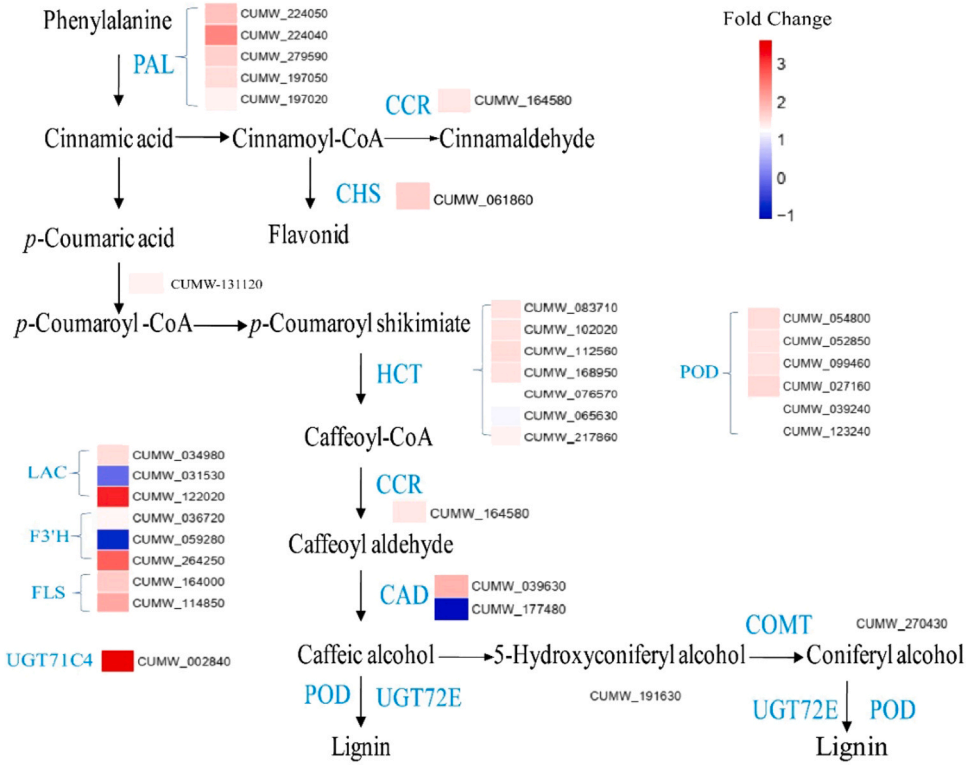

Fig. 9. Variations of 100 μL L^{-1} citral treatment at 12 h on expression patterns of differentially expressed genes (DEGs) involved in phenylpropanoid pathway. The rows in the heatmaps represent gene names, and the columns indicate samples. Fold change was distributed in the heatmap and the color scale from blue, through white, to red represents low, middle and high transcript levels, respectively.

Previous studies have shown that citral could potently inhibit growth of bacteria and fungi in postharvest melon, papaya and citrus fruit. At the same time, it can reduce fruit decay and maintain fruit quality (Fan et al., 2014; Luciano et al., 2023). In this work, we evaluated the preventative influence of citral as natural inducer to reduce citrus green mold. Citral fumigation effectively restrained development of green mold and reduced decay of citrus fruit (Fig. 2). The phenotypic response was not only related to direct antifungal activity of EOs but also the induced disease resistance of fruit. In particular, inducers promote the synthesis of secondary metabolites with antifungal activities in the fruit tissue, and this may have detrimental effects on the morphology and growth of fungi (Prusky and Romanazzi, 2023; Yang et al., 2016). The former was proved in our previous work (Zheng et al., 2015). The latter is generally thought to be related to the accumulation of secondary metabolites in the fruit peel and it is supported by our present study. In this study, citral exposure greatly improved the contents of total phenols, flavonoids and lignin and promoted their maximum accumulation on 3 or 4 d (Fig. 3). Increased contents of phenols and lignin would thus limit spread of *P. digitatum* into these healthy cells hence slowing down spread of green mold disease. Similar results have previously been reported by Li et al. (2020), suggesting that production of total phenols, flavonoids and lignin by 4-carvomenthenol effectively conferred disease resistance to *B. cinerea* in strawberry. In citrus fruit, *Pichia galeiformis* reduced the disease incidence and lesion diameter due to *P. digitatum* by improving the contents of total phenolic compounds, flavonoids, and lignin (Chen et al., 2021). Thus, the reduction in lesion size and fruit maceration observed after citral exposure may be attributable to its ability to enhance disease resistance of citrus fruit and the fungicidal activities of its derivatives. Untargeted metabolomics was further applied to explore the overall changes in metabolite profile and identify potential contributors of fruit resistance.

Plant secondary metabolites are known to act as triggers of plant defense response against pathogen infections (El Khetabi et al., 2022). These metabolites are closely associated with the observed fruit phenotype. Any change in metabolites can give an intuitive illustration to help identify the potential contributors to an observed phenotypic change (Yang et al., 2022). For instance, through metabolomic analysis, Li et al. (2020) found that 4-carvomenthenol induced resistance of "Hongyan" strawberry to *B. cinerea* by stimulating biosynthesis of phenylpropanoid and flavonoid. This led to accumulation of phenolics and flavonoids such as naringenin, cinnamaldehyde, coniferaldehyde, quercetin, and taxifolin. In a recent study, indoleacetic acid (IAA) treatment was suggested to be capable of enhancing resistance against *B. cinerea* by stimulating the pathways of phenylpropanoid, flavonoids, terpenoids and hormones to reduce kiwifruit gray mold (Li et al., 2023). Similarly, our metabolomics results showed that 11 phenylpropanoid metabolites namely coniferin, hesperidin, naringin, syringin, 7-methoxyflavonol, curcumin, camellianin, kaempferol-7-neohesperidoside, *trans*-cinnamaldehyde, cinnamyl alcohol, and vitexin-2-O-rhamnoside, markedly accumulated after exposure to citral (Figs. 4 and 5). These may have potentially contributed to the improvement in both antioxidant and antimicrobial activities (Duan et al., 2018; Wei et al., 2020), thus enhancing citrus defense to *P. digitatum*. For instance, curcumin was reported to directly decrease *B. cinerea* biomass, and promoted higher levels of H_2O_2 and defense-related genes in kiwifruit, helping to control gray mold (Kai et al., 2020). *Trans*-cinnamaldehyde was also observed in our previous study to directly inhibit *P. digitatum* and enhance disease resistance of citrus fruit (Duan et al., 2018). Additionally, syringin and coniferin have been associated with strengthening of plant cell walls (Passardi et al., 2004), which may explain our observed accumulation of lignin in citral-treated citrus peels (Fig. 3F). Particularly, we observed that syringin (lignin monomer) and hesperidin (a flavonoid) tremendously accumulated to $\log_2$ FC values of 11.11 and 8.95, respectively (Fig. 6B). These two are known to have great antioxidant and antifungal characteristics (Dadwal et al., 2022; Singh et al., 2020), and may be critical participants in the resistance enhancement by citral. As the same

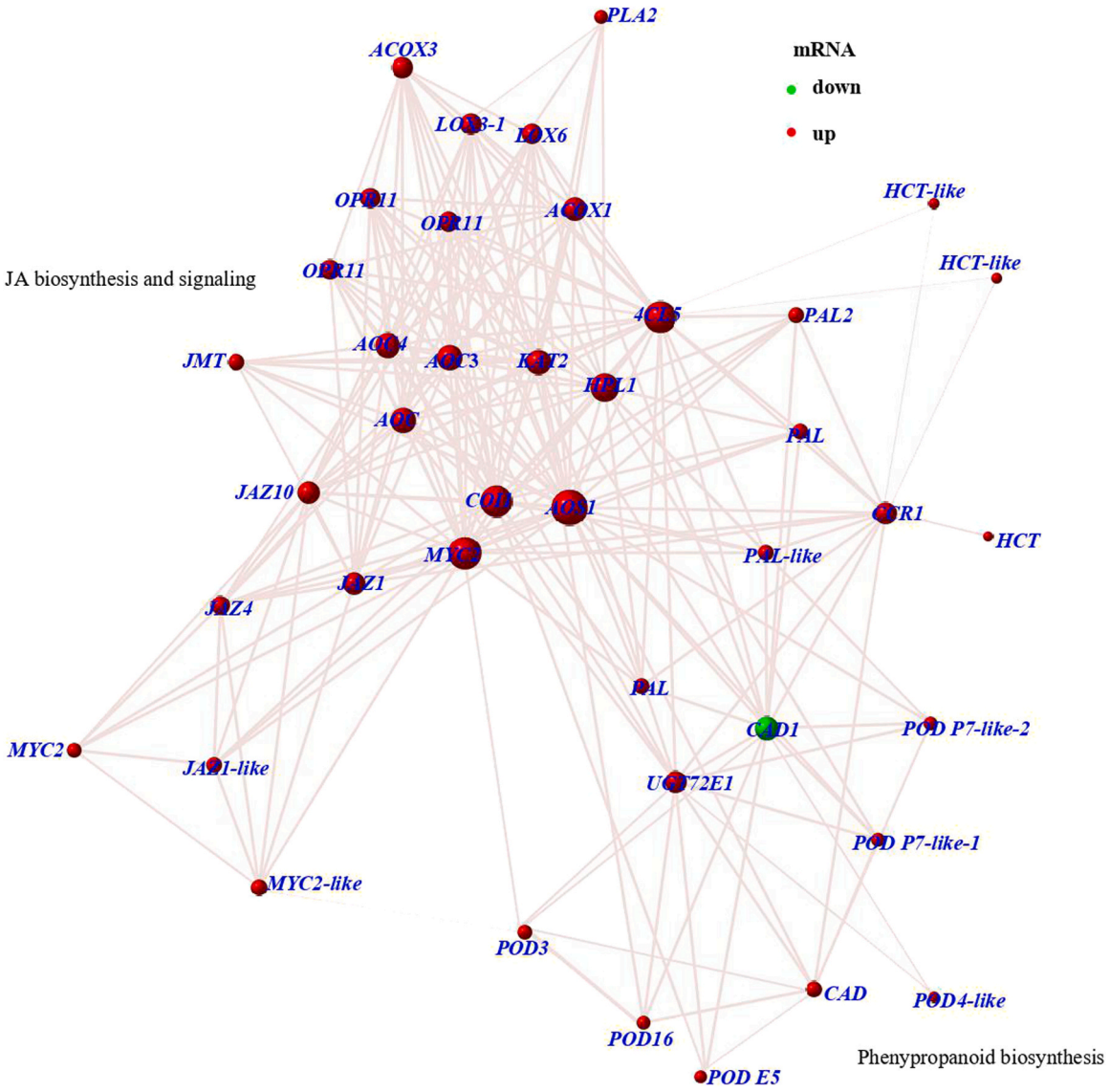

Fig. 10. Regulatory network of genes involved in JA biosynthesis, signaling and phenylpropanoid pathway in citrus fruit treated with 100 μL L^{-1} citral. Nodes represent 'genes' and lines represent 'relationships' between any two genes. Nodes colored in 'red' and 'blue' represent up- and down- regulation, respectively. The size of the nodes represents the correlation degree of the gene and it was determined by a Pearson correlation coefficient.

time, these results implied that citral exposure could reallocate the proportion of carbon sources in citrus peel, and specifically synthesize secondary metabolites, thereby improving the resistance of citrus fruit to *P. digitatum*. This also indicated the effect of citral on induced systemic resistance (ISR) of citrus fruit.

Metabolomics reveals the global changes in metabolites, while transcriptomics can provide evidence for all changes occurring in the fruit. In this study, we found that numerous genes involved in JA biosynthesis and signaling were predominantly induced in citral- treated peels. These genes are involved in the early rate-limiting steps, β-oxidation, and formation of JAs. LOX is an important enzyme that cleaves off the alpha-linolenic acid to generate 13(S)-HPOT in plants. Subsequently, 13(S)-HPOT is converted to 12-oxo-phytodienoic acid (12-OPDA) under the catalyzation of AOS and AOC (Li et al., 2021). The produced OPDA is transformed into JA by triple β-oxidation of OPR in peroxisome, and the derivative MeJA is finally converted through JMT (Fang et al., 2020). These genes are thus, critical in JA biosynthesis. We confirmed by qRT-PCR that the expression levels of *LOX2–1*, *AOC*, *AOS1*, *OPR11* and *JMT* were greatly increased in citral-treated peels. This suggested that the JA biosynthesis was activated, leading to accumulation of JA and MeJA (Fig. S3). Similar result was reported in benzothiadiazole treated apple (Deng et al., 2023), in which expression levels of *LOX*, *AOC*, *AOS*, *OPR* and *JMT* all increased, accompanied by increase in JA content. In addition, exogenous MeJA enhanced the activities and expression levels of *LOX*, *AOS*, and *OPR3*, accompanied by accumulated endogenous JA, thereby triggering defense response in peach fruit (Ji et al., 2021). By integrating metabolomic data, our results provided a closer connection between citral-treated citrus fruit and JA pathway. The metabolomic results showed that the contents of the phytohormones linolenic acid, ABA, IBA, IAA and MeJA greatly increased after citral treatment. These phytohormones do contribute to regulation networks of immunity by independently or synergistically inducing plant defense (Xu et al., 2022). The highest accumulation in our citral-treated samples was MeJA (Fig. 5), with level reaching 9.86-fold that in the control fruit, which might have enhanced the JA signal transduction.

Plant defense response against pathogens can be transferred by activating JA signaling, thus establishing ISR (Prusky and Romanazzi, 2023; Xu et al., 2022). If the JA signaling is intercepted, defense-related genes are unable to be stimulated, and ultimately leading to increased susceptibility to the pathogens. Three genes including *MYC2*, *JAZ*, and *COI* participate in JA signaling pathway, and they cooperate with each

other to regulate plant responses to external stresses (Min et al., 2020; Zhang et al., 2021). Valenzuela-Riffo et al. (2020) noted that MeJA application primed defense responses in strawberry by upregulating the expression levels of *JAZ1* and *MYC2*. In a recent research, mushroom alcohol activated JA biosynthesis and signaling to enhance sweet cherry resistance to *B. cinerea* (Li et al., 2022). Similarly, we observed increased expression levels of *JAZ1* and *MYC2* after citral treatment of citrus fruit. By contrast, the expression of *COI1* in the citral-treated samples was enhanced before 2 d and subsequently inhibited after 3 d (Fig. 8G). This phenomenon implied that the *COI1* potentially participated in the early defense response against *P. digitatum*. Similar result was reported by Liu et al. (2017), who found that the early up expression of *COI1* enhanced wheat resistance against *Blumeria graminis*. This result was, however, slightly different from a previous report in which the expression levels of *COI* was higher in test samples all through the experiment following exogenous treatment of strawberry with terpinen-4-ol (Li et al., 2021) and tomato with MeJA (Min et al., 2022). These data provide evidence that transcription of *COI1* may differ in defense response to different species. The combination of biochemical, metabolomics and transcriptomic analyses have given our more confidence that citral fumigation trigger JA pathway and therefore enhances citrus fruit resistance to *P. digitatum*.

Pathogens generally trigger a series of defense responses in plants, such as activation of Ca^{2+} sensors in cells, maintenance of redox balance, accumulation of antifungal substances, plant hormone signal transduction, etc (Yousuf et al., 2021). The hormone signaling appears to be important in controlling autophagy and plant stress responses (Liao and Bassham, 2020). A possible mechanism underlying JA-signaling-induced defense is that JA promotes the expression of defense-related genes and induce defense-related secondary metabolites, thereby enabling plant disease resistance to pathogen infection (Fonseca et al., 2009). As an important elicitor, JA can prime defense response by stimulating phenylpropanoid pathway in different fruit, thereby alleviating disease progression (Wang et al., 2021). A recent report demonstrated that silencing of JA signaling pathway reduced the contents of phenolic and flavonoid compound by blocking phenylpropanoid biosynthesis (Min et al., 2020). Three crucial enzymes (PAL, PPO, and POD) related to biosynthesis and oxidization of secondary metabolites, generally serve as defense-related enzymes for disease resistance assessment (Li et al., 2020). For instance, Pan et al. (2022) reported that MeJA induces disease resistance in sweet cherry fruit by improving the activities of PAL, POD, PPO, GLU and CHI and their gene expression. Our study also found that citral treatment increased the activities of PAL and POD. In contrast, PPO activity in citral-treated peels increased before 2 d and then was inhibited from 2 to 5 d. These changes were consistent with accumulation of total phenols, flavonoids, and lignin (Fig. 3). Similar observation was made in orange fruit, in which the activities of PAL and POD were stimulated after treatment with *Rhodosporidium paludigenum*, and PPO activity was markedly decreased after 36 h (Lu et al., 2013). Moreover, by transcriptomic analysis results, multiple transcripts involved in the phenylpropanoid metabolism pathways including *PAL, HCT, COMT, CCR, CHS, CAD, POD, PPO, FLS,* and *F3′H* showed higher expression levels after citral exposure (Fig. 9). At the same time, the transcripts involved in the JA pathway showed positive associations with phenylpropanoid biosynthesis-related genes (Fig. 10). The potential genes *MYC2*, *COI1* and *AOS1* positively correlated with the phenylpropanoid biosynthesis-related to genes (such as *PAL*, *PAL2*, *PAL-like*, and *4CL5*). They all indicated an important regulatory role of JA to secondary metabolic pathways in the citral treated citrus fruit. In particular, the relative expression of mostly genes involved in JA biosynthesis and signaling were enhanced before 3 d of exposure (Fig. 8). Taken together, our results suggest that citral treatment triggered JA biosynthesis and signaling, leading to mass accumulation of flavonoids and lignin after 3 or 4 d of exposure, and a subsequent enhancement of citrus fruit resistance to *P. digitatum*.

5. Conclusions

In conclusion, exposure of citrus fruit to citral can induce their resistance to *P. digitatum* and reduce postharvest fruit rot. This may be related to the ability of citral to induce JA biosynthesis and signal transduction of plant hormones, leading to upregulation of key genes. Furthermore, citral promotes production of phenylpropanoid compounds by upregulating the expression of genes involved in the phenylpropanoid pathway and increasing the activities of defense-related enzymes. Among them, syringin and hesperidin are potentially major contributors to the induced resistance, and the antifungal mechanism in vivo and in vitro should be further investigated in future research. This study provides novel perceptions into the resistance mechanism of citral controlling postharvest green mold.

CRediT authorship contribution statement

Bin Duan: Conceptualization, Methodology, Investigation, Writing – original draft. **Okwong Oketch Reymick**: Writing – review & editing. **Zhaoguo Liu:** Methodology, Data curation. **Yun Zhou:** Data curation. **Xin Wang:** Investigation, Validation. **Zhao Feng:** Investigation, Methodology. **Nengguo Tao:** Conceptualization, Writing – review & editing, Funding acquisition.

Declaration of Competing Interest

The authors declare that they have no known competing financial interests or personal relationships that could have appeared to influence the work reported in this paper.

Data availability

I have shared the link to my data at the Attach File step.

Acknowledgements

This study was supported by the National Natural Science Foundation of China (No. 32172253), the Natural Science Foundation of Hunan Province (2021JJ30666), and Guangdong Provincial Key Laboratory of Applied Botany, South China Botanical Garden, Chinese Academy of Sciences (No. AB202109).

Appendix A. Supporting information

Supplementary data associated with this article can be found in the online version at doi:10.1016/j.postharvbio.2023.112633.

References

Bhatta, U.K., 2022. Alternative management approaches of citrus diseases caused by *Penicillium digitatum* (green mold) and *Penicillium italicum* (blue mold). Front. Plant Sci. 12, 833328 https://doi.org/10.3389/fpls.2021.833328.

Chen, C., Cai, N., Chen, J., Wan, C., 2019. Clove essential oil as an alternative approach to control postharvest blue mold caused by *Penicillium italicum* in citrus fruit. Biomolecules 9, 197. https://doi.org/10.3390/biom9050197.

Chen, O., Deng, L., Ruan, C., Yi, L., Zeng, K., 2021. *Pichia galeiformis* induces resistance in postharvest citrus by activating the phenylpropanoid biosynthesis pathway[J]. J. Agric. Food Chem. 69 (8), 2619–2631. https://doi.org/10.1021/acs.jafc.0c06283.

Dadwal, V., Joshi, R., Gupta, M., 2022. A comparative metabolomic investigation in fruit sections of *Citrus medica* L. and *Citrus maxima* L. detecting potential bioactive metabolites using UHPLC-QTOF-IMS. Food Res. Int. 157, 111486 https://doi.org/10.1016/j.foodres.2022.111486.

Deng, H., Ma, L., Gong, D., Xue, S., Ackah, S., Prusky, D., Bi, Y., 2023. BTH-induced joint regulation of wound healing at the wounds of apple fruit by JA and its downstream transcription factors. Food Chem. 410, 135184 https://doi.org/10.1016/j.foodchem.2022.135184.

Duan, B., Gao, Z., Reymick, O.O., Ouyang, Q., Chen, Y., Long, C., Yang, B., Tao, N., 2021. Cinnamaldehyde promotes the defense response in postharvest citrus fruit inoculated with *Penicillium digitatum* and *Geotrichum citri-aurantii*. Pestic. Biochem. Phys. 179, 104976 https://doi.org/10.1016/j.pestbp.2021.104976.

Duan, X., OuYang, Q., Tao, N., 2018. Effect of applying cinnamaldehyde incorporated in wax on green mould decay in citrus fruits. J. Sci. Food Agr. 98, 527–533. https://doi.org/10.1002/jsfa.8490.

El Khetabi, A., Lahlali, R., Ezrari, S., Radouane, N., Lyousfi, N., Banani, H., Askarne, L., Tahiri, A., El Ghadraoui, L., Belmalha, S., Ait Barka, E., 2022. Role of plant extracts and essential oils in fighting against postharvest fruit pathogens and extending fruit shelf life: A review. Trends Food Sci. Tech. 120, 402–417. https://doi.org/10.1016/j.tifs.2022.01.009.

Fan, F., Tao, N., Lei, J., He, X., 2014. Use of citral incorporated in postharvest wax of citrus fruit as a botanical fungicide against *Penicillium digitatum*. Postharvest Biol. Technol. 90, 52–55. https://doi.org/10.1016/j.postharvbio.2013.12.005.

Fang, H., Luo, F., Li, P., Zhou, Q., Zhou, X., Wei, B., Cheng, S., Zhou, H., Ji, S., 2020. Potential of jasmonic acid (JA) in accelerating postharvest yellowing of broccoli by promoting its chlorophyll degradation. Food Chem. 309, 125737 https://doi.org/10.1016/j.foodchem.2019.125737.

Fonseca, S., Chico, J.M., Solano, R., 2009. The jasmonate pathway: the ligand, the receptor and the core signalling module. Curr. Opin. Plant Biol. 12, 539–547. https://doi.org/10.1016/j.pbi.2009.07.013.

Gong, M., Wang, Y., Su, E., Zhang, J., Tang, L., Li, Z., Zhang, L., Zou, G., Wan, J., Bao, D., 2022. The promising application of a β-glucosidase inhibitor in the postharvest management of *Volvariella volvacea*. Postharvest Biol. Technol. 185, 111784 https://doi.org/10.1016/j.postharvbio.2021.111784.

He, S., Ren, X., Lu, Y., Zhang, Y., Sun, L., 2016. Microemulsification of clove essential oil improves its in vitro and in vivo control of *Penicillium digitatum*. Food Control 65, 106–111. https://doi.org/10.1016/j.foodcont.2016.01.020.

Hyun, J., Lee, J.G., Yang, K., Lim, S., Lee, E.J., 2022. Postharvest fumigation of (*E*)-2-Hexenal on kiwifruit (*Actinidia chinensis* cv. 'Haegeum') enhances resistance to *Botrytis cinerea*. Postharvest Biol. Technol. 187, 111854 https://doi.org/10.1016/j.postharvbio.2022.111854.

Ji, N., Wang, J., Zuo, X., Li, Y., Zheng, Y., 2021. *PpWRKY45* is involved in methyl jasmonate primed disease resistance by enhancing the expression of jasmonate acid biosynthetic and pathogenesis-related genes of peach fruit. Postharvest Biol. Technol. 172, 111390 https://doi.org/10.1016/j.postharvbio.2020.111390.

Jiang, Y., Ji, X., Zhang, Y., Pan, X., Yang, Y., Li, Y., Guo, W., Wang, Y., Ma, Z., Lei, B., Yan, H., Liu, X., 2022. Citral induces plant systemic acquired resistance against tobacco mosaic virus and plant fungal diseases. Ind. Crop. Prod. 183, 114948 https://doi.org/10.1016/j.indcrop.2022.114948.

Kai, K., Hua, C., Sui, Y., Bi, W., Shi, W., Zhang, D., Ye, Y., 2020. Curcumin triggers the immunity response in kiwifruit against *Botrytis cinerea*. Sci. Hortic. 274, 109685 https://doi.org/10.1016/j.scienta.2020.109685.

Leng, L., Yuan, Z., Pan, R., Su, X., Wang, H., Xue, J., Zhuang, K., Gao, J., Chen, Z., Lin, H., Xie, W., Li, H., Chen, Z., Ren, K., Zhang, X., Wang, W., Jin, Z., Wu, S., Wang, X., Yuan, Z., Xu, H., Chow, H., Zhang, J., 2022. Microglial hexokinase 2 deficiency increases ATP generation through lipid metabolism leading to β-amyloid clearance. Nat. Metab. 4 (1420), 1287–1305. https://doi.org/10.1038/s42255-022-00682-x.

Li, G., Wang, Y., Zhang, Z., Chen, Y., Tian, S., 2022. Mushroom alcohol controls gray mold caused by *Botrytis cinerea* in harvested fruit via activating the genes involved in jasmonic acid signaling pathway. Postharvest Biol. Technol. 186, 111843 https://doi.org/10.1016/j.postharvbio.2022.111843.

Li, Z., Wang, N., Wei, Y., Zou, X., Jiang, S., Xu, F., Wang, H., Shao, X., 2020. Terpinen-4-ol enhances disease resistance of postharvest strawberry fruit more effectively than tea tree oil by activating the phenylpropanoid metabolism pathway. J. Agric. Food Chem. 68, 6739–6747. https://doi.org/10.1021/acs.jafc.0c01840.

Li, Z., Wei, Y., Cao, Z., Jiang, S., Chen, Y., Shao, X., 2021. The jasmonic acid signaling pathway is associated with Terpinen-4-ol-induced disease resistance against *Botrytis cinerea* in strawberry fruit. J. Agric. Food Chem. 69, 10678–10687. https://doi.org/10.1021/acs.jafc.1c04608.

Li, Z., Yang, S., Wang, X., Liao, Q., Zhang, W., Liu, J., Liu, G., Tang, J., 2023. Widely targeted metabolomics analysis reveals the effect of exogenous auxin on postharvest resistance to *Botrytis cinerea* in kiwifruit (*Actinidia chinensis* L.). Postharvest Biol. Technol. 195, 112129 https://doi.org/10.1016/j.postharvbio.2022.112129.

Liao, C., Bassham, D., C., 2020. Combating stress: the interplay between hormone signaling and autophagy in plants. J. Exp. Bot. 71 (5), 1723–1733. https://doi.org/10.1093/jxb/erz515.

Liu, X., Wang, J., Fan, B., Shang, Y., Sun, Y., Dang, C., Xie, C., Wang, Z., Peng, Y., 2017. A *COI1* gene in wheat contributes to the early defence response against wheat powdery mildew. J. Phytopathol. 166, 116–122. https://doi.org/10.1111/jph.12667.

Livak, K.J., Schmittgen, T., 2001. Analysis of relative gene expression data using real-time quantitative PCR and the $2^{-\triangle\triangle Ct}$ method. Methods 25 (4), 402–408. https://doi.org/10.1006/meth.2001.1262.

Lu, L., Ye, C., Guo, S., Sheng, K., Shao, L., Zhou, T., Yu, T., Zheng, X., 2013. Preharvest application of antagonistic yeast *Rhodosporidium paludigenum* induced resistance against postharvest diseases in mandarin orange. Biol. Control 67 (2), 130–136. https://doi.org/10.1016/j.biocontrol.2013.07.016.

Luciano, W.A., Pimentel, T.C., Bezerril, F.F., Barão, C.E., Marcolino, V.A., de Siqueira Ferraz Carvalho, R., dos Santos Lima, M., Martín-Belloso, O., Magnani, M., 2023. Effect of citral nanoemulsion on the inactivation of *Listeria monocytogenes* and sensory properties of fresh-cut melon and papaya during storage. Int. J. Food Microbiol. 384, 109959 https://doi.org/10.1016/j.ijfoodmicro.2022.109959.

Min, D., Li, F., Cui, X., Zuo, J., Li, Z., Ai, W., Shu, P., Zhang, X., Li, X., Meng, D., Guo, Y., Li, J., 2020. *SlMYC2* are required for methyl jasmonate-induced tomato fruit resistance to *Botrytis cinerea*. Food Chem. 310, 125901 https://doi.org/10.1016/j.foodchem.2019.125901.

Min, D., Li, Z., Fu, X., Li, F., Li, X., Zuo, J., Zhang, X., 2022. Autophagy is involved in methyl jasmonate-mediated resistance against *Botrytis cinerea* in postharvest tomato fruit by regulating jasmonate signaling and reactive oxygen species homeostasis. Sci. Hortic. 305, 111361 https://doi.org/10.1016/j.scienta.2022.111361.

Pan, L., Chen, X., Xu, W., Fan, S., Wan, T., Zhang, J., Cai, Y., 2022. Methyl jasmonate induces postharvest disease resistance to decay caused by *Alternaria alternata* in sweet cherry fruit. Sci. Hortic. 292, 110624 https://doi.org/10.1016/j.scienta.2021.110624.

Passardi, F., Penel, C., Dunand, C., 2004. Performing the paradoxical: how plant peroxidases modify the cell wall. Trends Plant Sci. 9 (11), 534–540. https://doi.org/10.1016/j.tplants.2004.09.002.

Prusky, D., Romanazzi, G., 2023. Induced resistance in fruit and vegetables: A host physiological response limiting postharvest disease development. Annu. Rev. Phytopathol. 61, 279–300. https://doi.org/10.1146/annurev-phyto-021722-035135.

Singh, B., Singh, J.P., Kaur, A., Singh, N., 2020. Phenolic composition, antioxidant potential and health benefits of citrus peel. Food Res. Int. 132, 109114 https://doi.org/10.1016/j.foodres.2020.109114.

Tamer, C.E., Suna, S., Özcan-Sinir, G., 2019. 14 - Toxicological aspects of ingredients used in nonalcoholic beverages. Non-Alcoholic Beverages. Woodhead Publishing,, pp. 441–481. https://doi.org/10.1016/B978-0-12-815270-6.00014-1.

Valenzuela-Riffo, F., Zuniga, P.E., Morales-Quintana, L., Lolas, M., Caceres, M., Figueroa, C.R., 2020. Priming of defense systems and upregulation of *MYC2* and *JAZ1* genes after *Botrytis cinerea* inoculation in methyl jasmonate-treated strawberry fruits. Plants 9 (4), 447. https://doi.org/10.3390/plants9040447.

Wang, F., Zhang, Z., Li, Q., Yu, T., Ma, C., 2020. Untargeted LC–MS/MS analysis reveals metabolomics feature of osteosarcoma stem cell response to methotrexate. Cancer Cell Int 20, 269. https://doi.org/10.1186/s12935-020-01356-y.

Wang, H., Liu, Z., Wang, S., Cui, D., Zhang, X., Liu, Y., Zhang, Y., 2017. UHPLC-Q-TOF/MS based plasma metabolomics reveals the metabolic perturbations by manganese exposure in rat models. Metallomics 9 (2), 192–203. https://doi.org/10.1039/C7MT00007C.

Wang, S., Shi, X., Liu, F., Laborda, P., 2021. Effects of exogenous methyl jasmonate on quality and preservation of postharvest fruits: A review. Food Chem. 353 (3), 129482 https://doi.org/10.1016/j.foodchem.2021.129482.

Wang, X., Zhu, J., Wei, H., Ding, Z., Li, X., Liu, Z., Wang, H., Wang, Y., 2023. Biological control efficacy of *Bacillus licheniformis* HG03 against soft rot disease of postharvest peach. Food Control 145, 109402. https://doi.org/10.1016/j.foodcont.2022.109402.

Wei, C., Zhang, F., Song, L., Chen, X., Meng, X., 2020. Photosensitization effect of curcumin for controlling plant pathogen *Botrytis cinerea* in postharvest apple. Food Control 123 (2), 107683. https://doi.org/10.1016/j.foodcont.2020.107683.

Wuryatmo, E., Able, A.J., Ford, C.M., Scott, E.S., 2014. Effect of volatile citral on the development of blue mould, green mould and sour rot on navel orange. Australas. Plant Path. 43 (4), 403–411. https://doi.org/10.1007/s13313-014-0281-z.

Xu, X., Chen, Y., Li, B., Zhang, Z., Qin, G., Chen, T., Tian, S., 2022. Molecular mechanisms underlying multi-level defense responses of horticultural crops to fungal pathogens. Hortic. Res. 9, uhac066 https://doi.org/10.1093/hr/uhac066.

Yang, S., Liu, L., Li, D., Xia, H., Su, X., Peng, L., Pan, S., 2016. Use of active extracts of poplar buds against Penicillium italicum and possible modes of action. Food Chem. 196, 610–618. https://doi.org/10.1016/j.foodchem.2015.09.101.

Yang, R., Miao, J., Chen, X., Chen, C., Simal-Gandara, J., Chen, J., Wan, C., 2022. Essential oils nano-emulsion confers resistance against *Penicillium digitatum* in 'Newhall' navel orange by promoting phenylpropanoid metabolism. Ind. Crop. Prod. 187, 115297 https://doi.org/10.1016/j.indcrop.2022.115297.

Yousuf, B., Wu, S., Siddiqui, M.W., 2021. Incorporating essential oils or compounds derived thereof into edible coatings: effect on quality and shelf life of fresh/fresh-cut produce. Trend Food Sci. Tech. 108, 245–257. https://doi.org/10.1016/j.tifs.2021.01.016.

Zhang, L., Wang, L., Zeng, X., Chen, R., Yang, S., Pan, S., 2019. Comparative transcriptome analysis reveals fruit discoloration mechanisms in postharvest strawberries in response to high ambient temperature. Food Chem. X 2, 100025. https://doi.org/10.1016/j.fochx.2019.100025.

Zhang, P., Jia, H., Gong, P., Sadeghnezhad, E., Pang, Q., Dong, T., Li, T., Jin, H., Fang, J., 2021. Chitosan induces jasmonic acid production leading to resistance of ripened fruit against *Botrytis cinerea* infection. Food Chem. 337, 127772 https://doi.org/10.1016/j.foodchem.2020.127772.

Zhao, L., He, F., Li, B., Gu, X., Zhang, X., Dhanasekaran, S., Zhang, H., 2022. Transcriptomic analysis of the mechanisms involved in enhanced antagonistic efficacy of *Meyerozyma guilliermondii* by methyl jasmonate and disease resistance of postharvest apples. LWT-Food Sci. Technol. 160, 113323 https://doi.org/10.1016/j.lwt.2022.113323.

Zheng, S., Jing, G., Wang, X., Ouyang, Q., Jia, L., Tao, N., 2015. Citral exerts its antifungal activity against *Penicillium digitatum* by affecting the mitochondrial morphology and function. Food Chem. 178, 76–81. https://doi.org/10.1016/j.foodchem.2015.01.077.

Zhi, H., Zhang, C., 2013. Effects of endogenous abscisic acid, jasmonic acid, polyamines, and polyamine oxidase activity in tomato seedlings under drought stress. Sci. Hortic. 159 (4), 172–177. https://doi.org/10.1016/j.scienta.2013.05.013.